$N(^4S_{3/2})$ Reaction with NO and NO_2: Temperature Dependent Rate Coefficients and $O(^3P)$ Product Yield

Dimitrios K. Papanastasiou[1,2], Jeremy Bourgalais[1,2], Tomasz Gierczak[1,2,#] and James B. Burkholder[1]

[1] Earth System Research Laboratory, Chemical Sciences Division, National Oceanic and Atmospheric Administration, 325 Broadway, Boulder, CO 80305-3328
[2] Cooperative Institute for Research in Environmental Sciences, University of Colorado, Boulder, CO 80309

Permanent address: Department of Chemistry, Warsaw University, al. Zwirki i Wigury 101, 02-089 Warszawa, Poland

Running Title: $N(^4S_{3/2})$ Reaction with NO and NO_2

*Corresponding author: James B. Burkholder
e-mail: James.B.Burkholder@noaa.gov
ORCID: 0000-0001-9532-6246
Phone: (303)-497-3252

Abstract

The $N(^4S_{3/2})$ + NO (k_1) and $N(^4S_{3/2})$ + NO_2 (k_2) gas-phase reactions, relevant to upper-atmospheric NO_x chemistry, were studied using a discharge flow tube reactor with atomic resonance fluorescence detection of $O(^3P)$ atoms. Reaction rate coefficients were measured over the temperature range 216–344 K to be $k_1(T) = (2.61 \pm 0.19) \times 10^{-11} \exp((86 \pm 21)/T)$ and $k_2(T) = (2.41 \pm 0.62) \times 10^{-12} \exp((442 \pm 64)/T)$ cm^3 molecule^{-1} s^{-1}. The $O(^3P)$ yield in the NO_2 reaction was found to be 0.66 ± 0.06. Our results are compared with previous studies and rate coefficient recommendations are provided.

1. Introduction

Nitrogen oxides, NO and NO_2, play a key role in processes within the field of planetary atmospheric chemistry, combustion, and astrochemistry [1-5]. In Earth's upper stratosphere and mesosphere, the abundance and partitioning of NO and NO_2 is primarily determined via their reaction with ground electronic state nitrogen atoms, $N(^4S_{3/2})$ [1,2]. The reaction of $N(^4S_{3/2})$ with NO also controls NO abundance in the Martian and Venusian atmosphere and in interstellar clouds [3-5]:

$$N(^4S_{3/2}) + NO(X^2\Pi) \rightarrow N_2 + O(^3P) \qquad \Delta H_r(298\ K) = -75.1\ kcal\ mol^{-1} \qquad (1)$$

with $\Delta H_0(298\ K)$ values taken from Burkholder et al. [6].

The rate coefficient for reaction 1, $k_1(T)$, has been measured numerous times [3,7-19], mostly near room temperature, but the agreement among the studies is poor. The NASA/JPL data evaluation recommends $k_1(T) = 2.1 \times 10^{-11} \exp(100/T)$ cm^3 molecule^{-1} s^{-1}, between 196 and 400 K, with an 1σ uncertainty factor of 30% that reflects the large spread in the reported values. The recommendation is based primarily on the work of Lee et al. [14] and Wennberg et al. [19], while the more recent studies of Nakayama et al. [16] and Bergeat et al. [3] were not available at the time of evaluation. Wennberg et al. employed a discharge flow reactor with resonance fluorescence (RF) detection of $N(^4S_{3/2})$ and reported $k_1(213–369\ K) = (2.2 \pm 0.2) \times 10^{-11} \exp[(160 \pm 50)/T]$ cm^3 molecule^{-1} s^{-1}. Lee et al. used both discharge-flow and flash-photolysis techniques with RF detection of $N(^4S_{3/2})$ and report $k_1(196–400\ K) = (3.4 \pm 0.9) \times 10^{-11}$ cm^3 molecule^{-1} s^{-1}. Nakayama et al. [16] used laser-induced fluorescence detection of $N(^4S_{3/2})$ and reported $k_1(295\ K) = (3.8 \pm 0.2) \times 10^{-11}$ cm^3 molecule^{-1} s^{-1}. Bergeat et al. [3] studied reaction 1

between 48 and 211 K in a supersonic flow reactor with RF detection of $N(^4S_{3/2})$ and report $k_1(211\ K) = (3.3 \pm 0.2) \times 10^{-11}$ cm^3 molecule^{-1} s^{-1} (1σ uncertainty).

The reaction of $N(^4S_{3/2})$ with ground-state $NO_2(^2A_1)$, has four energetically accessible product channels:

$$N(^4S_{3/2}) + NO_2 \rightarrow N_2O + O(^3P) \qquad \Delta H_r(298\ K) = -41.9 \text{ kcal mol}^{-1} \qquad (2a)$$

$$\rightarrow N_2 + O_2 \qquad \Delta H_r(298\ K) = -121.0 \text{ kcal mol}^{-1} \qquad (2b)$$

$$\rightarrow NO + NO \qquad \Delta H_r(298\ K) = -77.5 \text{ kcal mol}^{-1} \qquad (2c)$$

$$\rightarrow N_2 + O(^3P) + O(^3P) \qquad \Delta H_r(298\ K) = -1.9 \text{ kcal mol}^{-1} \qquad (2d)$$

while channel 2d is spin forbidden. $k_2(T)$ has been reported in several studies [9,11,16,19-21], but the agreement is poor. The NASA/JPL data evaluation recommends $k_2(T) = 5.8 \times 10^{-12} \exp(220/T)$ cm^3 molecule^{-1} s^{-1} with a 1σ uncertainty factor of 50% at 298 K, which encompasses the spread in the reported values. The recommendation is based on the work of Wennberg et al. [19] who employed the same experimental approach as in reaction 1. Nakayama et al. [16] also studied the NO_2 reaction and reported $k_2(295\ K)$ to be ~40% less than reported by Wennberg et al. The studies of Clyne and McDermid [9] and Wennberg et al. [19] suggest that reaction 2 leads almost exclusively to N_2O and $O(^3P)$ production, but can't rule out a significant branching ratio for channels 2b and/or 2c. Although the Kistiakowsky and Vopli [13] study of reaction 2 is mostly qualitative, the authors conclude that channels 2a-2c are active. In contrast to other studies, Phillips and Schiff [21] concluded that channel 2d contributes to the overall reaction with a yield of 0.13 ± 0.11. Zuo et al. [22] explored the reaction mechanism theoretically and found that the initial formation of an N-NO_2 adduct leads to channels 2a-2c via submerged transition states, which makes these channels open even at low temperatures.

The large discrepancies among the available studies of $k_1(T)$ and $k_2(T)$ highlights the need for further investigation of these reactions and potential reduction of rate coefficient uncertainty in atmospheric chemistry models. In addition, the branching ratio for reaction 2 has not been well characterized. In this study, a discharge flow reactor coupled with resonance fluorescence detection of $O(^3P)$ atoms was used to measure $k_1(T)$ and $k_2(T)$ at temperatures between 216 and 344 K. The $O(^3P)$ product detection enables a more complete understanding of $k_2(T)$ and product channel branching ratios.

2. Experimental details

A discharge flow reactor coupled with resonance fluorescence atom detection has been used previously in this laboratory [23-25] and only details relevant to the present study are given here. The setup consists of i) a discharge flow tube reactor with a movable injector, ii) a microwave discharge resonance lamp for $O(^3P)$ excitation, and iii) a solar blind photomultiplier tube for detection of $O(^3P)$ atom fluorescence at 131 nm.

The jacketed cylindrical flow reactor has an I.D. of ~2.5 cm. The reactor was temperature controlled (±1 K) by circulating a temperature regulated fluid through its jacket. The carrier gas, He or N_2, mixed with the flow of N atoms generated in a microwave discharge source mounted on a side-arm of the flow reactor. NO or NO_2 flowed through a movable Pyrex injector (6 mm O.D.) centered in the flow tube. $O(^3P)$ was monitored at different reaction times by varying the injector's position, 0 to 30 cm, relative to the resonance fluorescence detection region. The flow tube pressure was measured in the middle of the reaction region and was in the 2 to 5.6 Torr range over the course of the study. The temperature of the reactor was monitored in the center of the flow tube with a retractable thermocouple. The total gas flow was in the range 9.6-24.4 $cm^3\ s^{-1}$ (standard temperature and pressure, STP) with linear gas flow velocities in the flow tube between 435 and 1032 $cm\ s^{-1}$. The walls of the flow tube were covered by a Teflon sheet (<1 mm thick) to reduce $O(^3P)$ and $N(^4S_{3/2})$ atom wall loss.

Ground-state N atoms, $N(^4S_{3/2})$, were generated by flowing ~400 ppm of N_2 in He through a 10 W microwave discharge at a total gas flow of ~0.17 $cm^3\ s^{-1}$ (STP). Experiments were performed with different carrier gases (He or N_2) and with efficient quenching partners, e.g. O_2, Cl_2 or SF_6, added to the flow to evaluate possible kinetic interference from excited states of N, $N(^2D)$ or $N(^2P)$.

$O(^3P)$ atom detection was achieved by resonance fluorescence detection upon excitation at its $^3S_1 \leftarrow {}^3P_J$ transition at 131 nm. A 20 W microwave discharge lamp, operated at ~2 Torr and with a 0.23 $cm^3\ s^{-1}$ (STP) flow of UHP He, was used as the source. The VUV radiation from the discharge lamp passed through a CaF_2 window, to minimize Lyman-α and N atom radiation detection. Fluorescence was collected using a MgF_2 lens (~10 cm focal length at 131 nm) and detected by a solar blind PMT (115–200 nm range) mounted perpendicular to the discharge lamp and flow tube. Wood's horns mounted opposite of the discharge lamp and PMT minimized detection of scattered background radiation. A 10 μs photon counting bin size and an average of ~5000 points was used for data acquisition. The detection limit (S/N=1, 1 s integration) at 2 Torr

reactor pressure was typically ~0.5 and ~1 × 10^9 atom cm^{-3} in He and N_2 carrier gas, respectively.

k_1(T) was measured under pseudo first-order conditions in NO, i.e., [NO] > [N($^4S_{3/2}$)]. The O(^{3}P) reaction profile was described by:

$$S_t = S_0 \cdot e^{-k_w \cdot (t-t_0)} + \left(\frac{S_{max} \cdot k_1'}{k_w - k_1'}\right) \cdot \left(e^{-k_1' \cdot (t-t_0)} - e^{-k_w \cdot (t-t_0)}\right) \quad \text{(I)}$$

where its production, reaction 1, is given by the pseudo first-order rate coefficient $k_1' = k_1$[NO], and k_w represents its first-order wall loss rate coefficient. S_t and S_0 are the O(^{3}P) fluorescence signal (proportional to [O(^{3}P)]) at reaction time t and time zero (t_0), i.e., background O(^{3}P) signal. S_{max} is the maximum O(^{3}P) fluorescence signal that is proportional to the initial N($^4S_{3/2}$) atom concentration. S_{max} was determined separately for each measured time profile by titrating N($^4S_{3/2}$) to O(^{3}P) with excess [NO]. The initial N atom concentration, $[N]_0$, was estimated from the O atom sensitivity and S_{max}. The O atom sensitivity was determined by partial titration of N($^4S_{3/2}$) with known amounts of NO. The measurements are corrected for background scattered light contributions. O(^{3}P) reaction profiles were fit to eq. I to obtain k_1' and k_w with S_0, S_{max}, and t_0 constrained to measured values. In all cases, k_w was <2 s^{-1} and statistically insignificant and had a negligible impact on the determination of k_1(T).

k_2(T) was measured under pseudo first-order conditions in NO_2. The measured O(^{3}P) profile was described by its production, reaction 2, with a pseudo first-order rate coefficient $k_2' = k_2$[NO_2] and branching yield Φ, and a loss via:

$$O(^3P) + NO_2 \rightarrow NO + O_2 \quad (3)$$

k_3(T) is well-established with $k_3(T) = 5.1 \times 10^{-12} \exp(210/T)$ cm^3 $molecule^{-1}$ s^{-1} [6]. Under the low-pressure conditions of our experiments, the O(^{3}P) + NO_2 + M association reaction is negligible. The O(^{3}P) temporal profile was described as:

$$S_t = S_0 \cdot e^{-k_3' \cdot (t-t_0)} + \left(\frac{S_{max} \cdot \Phi \cdot k_2'}{k_3' - k_2'}\right) \cdot \left(e^{-k_2' \cdot (t-t_0)} - e^{-k_3' \cdot (t-t_0)}\right) \quad \text{(II)}$$

where k_3' is the first-order loss of O(^{3}P) due to reaction 3, $k_3' = k_3$[NO_2]. O(^{3}P) reaction profiles were fit to eq. II to determine k_2' and Φ with k_3', S_0, S_{max}, and t_0 constrained by experimental measurements. O(^{3}P) wall loss rate was insignificant and neglected here.

The O(^{3}P) fluorescence signal was measured as a function of injector position, i.e., reaction time, typically 6–7 reaction times, for a given [NO] or [NO_2]. The maximum reaction time was ~50 ms. The background scattered light signal was measured without the reactant

present in the flow reactor and the N atom source microwave discharge off. The maximum $O(^3P)$ fluorescence signal, S_{max}, was measured by titrating $N(^4S_{3/2})$ atoms with excess of NO. Background $O(^3P)$ levels ranged between (1.0–4.0) × 10^{10} atoms cm^{-3}. The procedure was repeated for a range of [NO] or [NO_2].

The fitted k_1' and k_2' values were corrected for axial diffusion [19,23,26] and the corrections were always <3%. k_1(T) and k_2(T) were determined at each temperature by a weighted linear least-squares fit of k_1' versus [NO] and k_2' versus [NO_2].

2.1 Materials

For the NO reaction measurements, a 2047 (± 41) ppmv NO/N_2 gas mixture was used as supplied. The concentration of NO in the reactor was determined using calibrated flow meters and the NO gas mixture composition. The gas mixture had a stated NO_2 impurity of 13 ppmv, which made a negligible contribution to the measured k_1(T). For the NO_2 reaction measurements, a 1.67% NO_2/He mixture was prepared manometrically in a 12 L glass bulb. [NO_2] was determined from measured flows, $\Delta P/\Delta t$, of the mixture. SF_6 (99.99%) and a 5% Cl_2/N_2 gas mixture were used as supplied. The flow of He (UHP, 99.999%) was passed through a molecular sieve trap held at ~77 K to reduce discharge background levels of H or O atoms as well as background radiation detected by the PMT. N_2 and synthetic air (UHP, 99.999%) were used as supplied. Pressures were measured using 10, 100, and 1000 Torr capacitance manometers. Gas flows were measured using calibrated flow meters. All uncertainties quoted here are at the 2σ (95% confidence) level, unless stated otherwise.

3. Results and discussion

3.1 $N(^4S_{3/2})$ + NO reaction

k_1(T) was measured between 225 and 344 K at pressures in the 2.1 to 5.6 Torr (N_2) range. A summary of the measurement conditions and the obtained k_1(T) values is given in **Table 1**. Representative $O(^3P)$ reaction profiles are given in **Fig. 1**. For all experimental conditions, the $O(^3P)$ profiles were well represented by eq. I. Numerical kinetic simulations of the system confirmed that even for the lowest [NO]/[$N(^4S_{3/2})$] ratio employed in this study, eq. I accurately described the $O(^3P)$ temporal profiles to within the measurement uncertainty.

Fig. 1 also shows a summary of k_1'(296 K) versus [NO]. k_1(296 K) was measured to be (3.36 ± 0.04) × 10^{-11} cm^3 $molecule^{-1}$ s^{-1}, where the uncertainty is the fit precision. Plots of k_1'(T)

vs. [NO] obtained at the other temperatures in this work are provided in the Supplementary Information. Variation in flow velocity or initial [$N(^4S_{3/2})$] had a negligible effect on the rate coefficient measurement. In addition, no rate coefficient pressure, or bath gas (N_2 or He), dependence was observed between 2.1 and 5.6 Torr.

Fig. 2 shows k_1(225–344 K) measured in this work, where a slight negative temperature dependence, is observed, E/R = -(86 ± 21) K. k_1(T) is well described with the Arrhenius expression $k_1(T) = (2.61 \pm 0.19) \times 10^{-11} \exp((86 \pm 21)/T)$ cm^3 molecule^{-1} s^{-1}, where the quoted uncertainty is the fit precision.

The presence of metastable N atoms, $N(^2D)$ and/or $N(^2P)$, generated in the microwave discharge source and their subsequent reaction with NO, a possible source of error in previous studies, was investigated by the addition of efficient quenchers to the gas flow [18]. The 298 K quenching rate coefficient of $N(^2D)$ to ground-state $N(^4S)$ by N_2 and He are 1.3×10^{-14} and 4.6×10^{-17} cm^3 molecule^{-1} s^{-1}, respectively. There was, therefore, sufficient time to collisionally quench metastable N atoms, >99%, by N_2 before mixing with NO or NO_2 in the flow tube. In a separate experiment, He (~4 Torr) was used as the carrier gas and k_1(296 K) was found to be in good agreement, to within 5%, with the results obtained with N_2 as the carrier gas. In several experiments, O_2 was also added in the gas flow, (3.5–5.3) × 10^{14} molecule cm^{-3}, to quench metastable N atoms and secondary chemistry. Under these conditions, O_2 reacts with $N(^2D)$, 1.4×10^{-11} cm^3 molecule^{-1} s^{-1} [27], to produce NO and $O(^3P)$ in <1 ms:

$$N(^2D) + O_2 \rightarrow NO + O(^3P) \quad (4)$$

The addition of O_2 before the N atom source output mixed with NO in the flow tube had a negligible effect on the measured k_1(T) at all temperatures in this study. In summary, metastable N atoms possibly produced in the discharge source, were either rapidly quenched to $N(^4S)$ or reacted away without any complication to the measured $O(^3P)$ reaction profile and kinetic analysis.

3.2 $N(^4S_{3/2})$ + NO_2 reaction

k_2(T) was measured between 216 and 296 K at pressures in the range 2.0 to 4.1 Torr (He). **Table 2** includes a summary of the experimental conditions and the obtained k_2(T) and $O(^3P)$ yields, Φ. Representative $O(^3P)$ reaction profiles are shown in **Fig. 3** for different [NO_2]. The $O(^3P)$ profiles were well represented by eq. II, under all experimental conditions.

Fig. 3 also includes a summary of k_2'(296 K) data versus [NO_2]. A linear least-squares fit results in k_2(296 K) = (1.10 ± 0.06) × 10^{-11} cm^3 $molecule^{-1}$ s^{-1}, where the uncertainty is the fit precision. Second-order plots obtained at other temperatures are included in the supplement. Variation in flow velocity or initial [$N(^4S_{3/2})$] had a negligible effect on the obtained k_2'(T) and $O(^3P)$ yield. There was no observed k_2'(T) or $O(^3P)$ yield pressure dependence. Although Iwata et al.[28] have shown that $N(^2D)$ and $N(^2P)$ do not react rapidly with NO_2, all experiments were performed with O_2 added to the gas stream. Replacing O_2 with SF_6, another efficient quencher for metastable atoms, yielded indistinguishable results to within the measurement precision.

Figure 4 shows k_2(T) measured in this work at temperatures within 216 and 295 K where a negative temperature dependence is observed, E/R = -(442 ± 64) K. k_2(T) is well described with the Arrhenius expression $k_2(T) = (2.41 \pm 0.62) \times 10^{-12} \exp((442 \pm 64)/T)$ cm^3 $molecule^{-1}$ s^{-1}, where the quoted uncertainty is the fit precision.

The discharge source could also produce H-atoms that can potentially systematically bias our kinetic and yield measurements via the following sequence of catalytic reactions [29]:

$$H + NO_2 \rightarrow OH + NO \qquad k(298\ K) = 1.3 \times 10^{-10}\ cm^3\ molecule^{-1}\ s^{-1} \qquad (5)$$

$$N(^4S_{3/2}) + OH \rightarrow NO + H \qquad k(298\ K) = 5.8 \times 10^{-11}\ cm^3\ molecule^{-1}\ s^{-1} \qquad (6)$$

In a separate experiment, 1.5 × 10^{14} molecule cm^{-3} of Cl_2 was added to scavenge H-atoms (k(298 K) = 1.97 × 10^{-11} cm^3 $molecule^{-1}$ s^{-1} [29]), if present, in less than 1 ms, i.e., before the N-atom gas flow interacts with NO_2. k_2(296 K) obtained in the presence of Cl_2 agreed, to within the measurement uncertainty of ~10%, with our other 296 K measurements. This implies that H-atom production in the radical source did not impact our k_2(T) determination.

The NO produced via reaction 3, and possibly channel 2c, could possibly interfere with our kinetic and $O(^3P)$ yield analysis due to its secondary reaction with $N(^4S_{3/2})$, reaction 1. Numerical simulations of the reaction system were performed for the conditions given in **Table 2** and [$N(^4S_{3/2})$] = 3 × 10^{11} molecule cm^{-3} and [NO_2] = (2–8) × 10^{12} molecule cm^{-3}. The results showed that a systematic deviation in the $O(^3P)$ reaction profiles only occurred for high [NO_2] conditions at long reaction times, >35 ms, where [NO] increased significantly. Therefore, the contribution of secondary $O(^3P)$ production under our experimental conditions was not significant within our measurement uncertainty.

Table 2 includes the $O(^3P)$ yield results that show that $O(^3P)$ is formed with the same yield at all the temperatures of this study, to within the measurement precision. We report a temperature independent $O(^3P)$ yield of 0.66 ± 0.02 over the temperature range 216–296 K, from a weighted average of all the measurements.

3.3. Uncertainty Analysis

The absolute uncertainty of the kinetic measurements is associated with the measurement precision of the $O(^3P)$ fluorescence signal, $O(^3P)$ profile fits, the precision of the second-order rate coefficient fits, and contributions from systematic errors. In addition, the uncertainty in [NO] and [NO_2] contributes to the absolute uncertainty. The measurement precision of the $O(^3P)$ fluorescence signal was ~3%. The $O(^3P)$ profile fits to eqs I and II was always better than <4%. The precision of the second-order fits was ~5% for reaction 1 and ~7% for the NO_2 reaction. [NO] and [NO_2] was determined by measurements of gas flows, pressure and temperature in the reactor, as well as the mixing ratio of the NO/N_2 and NO_2/He gas mixture. The uncertainty in [NO] and [NO_2] is estimated to be ~6%. The presence of metastable N-atoms or impurities from the discharge source was systematically explored and found to have a negligible influence in the present study. In addition, numerical kinetic simulations showed that the pseudo first-order approximation as well as unwanted secondary chemistry did not affect our results to within the measurement uncertainty. The total uncertainty in k_1(T) and k_2(T) is estimated to be ~8-10%. The overall uncertainty of the $O(^3P)$ yield is estimated to be ~9%.

3.4 Comparison with previous studies

Fig. 2 includes a comparison of k_1(T) measured in this work with previous results and the NASA/JPL recommendation [6]. Wennberg et al., Nakayama et al., and the NASA/JPL data evaluation provide in-depth discussions of earlier studies and plausible explanations for discrepancies in the kinetic results that will not be repeated here. We will focus our discussion on the preferred study of Wennberg et al. and the more recent study by Nakayama et al. Wennberg et al. employed a discharge flow technique with resonance fluorescence detection similar to the approach used in our study. Their k_1(298 K) determination of (3.6 ± 0.4) × 10^{-11} cm^3 $molecule^{-1}$ s^{-1} is ~9% greater than our 296 K value, but falls well within the combined estimated uncertainty of the studies. k_1(T) from Wennberg et al. shows a steeper temperature dependence, E/R = -(160 ± 50) K, than found here, E/R = -(86 ± 21) K which is nearly within the

combined measurement uncertainty. Nakayama et al. utilized a pulsed laser photolysis-laser induced fluorescence (PLP-LIF) method and report k_1(295 K) = (3.8 ± 0.2) × 10^{-11} cm^3 $molecule^{-1}$ s^{-1}, which is ~13% greater than our 296 K value. Although the 211 K measurement from Bergeat et al. [3] is outside our measurement temperature range, their k_1(211 K) is ~16% lower than what our Arrhenius fit would predict, but within the combined measurement uncertainty. Lee et al. [14] used two independent techniques, discharge-flow and flash-photolysis techniques with RF detection of $N(^4S_{3/2})$, and reported a temperature-independent rate coefficient k_1(196–400 K) = (3.4 ± 0.9) × 10^{-11} cm^3 $molecule^{-1}$ s^{-1}. However, the agreement between the two approaches was poor, which led to a reported large uncertainty. Therefore, the results of Lee et al. are not considered further.

The NASA/JPL [6] recommendation for reaction 1 is an average from the work of Wennberg et al. and Lee et al. [14], where the recommended uncertainty, 30% (1σ) at 298 K, covers the spread of all the previous studies. The recommended k_1(298 K) = (3.0 ± 0.6) × 10^{-11} cm^3 $molecule^{-1}$ s^{-1} is ~10% lower than our work and ~20% from that of Wennberg et al., while the recommended temperature dependence, E/R = -100 K, is in excellent agreement with the results from this work. Our study and that of Wennberg et al, report thorough investigations of possible systematic interferences from metastable N atoms or impurities from the discharge source, a common problem in previous studies. In addition, the work of Nakayama et al. confirms the room-temperature results from Wennberg et al. and this work. Therefore, we have combined the results from this work, Wennberg et al., and Nakayama et. al., to report k_1(298 K) = (3.60 ± 0.52) × 10^{-11} cm^3 $molecule^{-1}$ s^{-1} and k_1(213–369 K) = 2.31 × 10^{-11} exp(134/T) cm^3 $molecule^{-1}$ s^{-1} with uncertainty factors of f(298 K) = 1.07 and g = 30. The recommended k_1(T) is included in **Fig. 2**.

Fig. 4 compares k_2(T) from our work with results from previous studies and the NASA/JPL [6] recommendation. We focus our discussion on the recommended Wennberg et al. study and the more recent Nakayama et al. study. Wennberg et al. report k_2(298 K) = (1.2 ± 0.1) × 10^{-11} cm^3 $molecule^{-1}$ s^{-1}, which is in good agreement, to within 9 %, with our 296 K result. Wennberg et al. measured a lower temperature dependence, E/R = -(220 ± 50) K, as compared to E/R = -(442 ± 64) K from our study. Nakayama et al. reported k_2(295 K) = (7.8 ± 0.9) × 10^{-12} cm^3 $molecule^{-1}$ s^{-1}, which is ~28% less than our k_2(296 K) value of (1.10 ± 0.09) × 10^{-11} cm^3 $molecule^{-1}$ s^{-1}. The source of this discrepancy is not presently understood, however the second-

298 order plot presented in the Nakayama et al. appears to show a systematic underestimation in k_2
299 with increasing NO_2 that may account for the discrepancy.

300 We suggest that the good agreement between this study and the results of Wennberg et
301 al., over a fairly broad overlapping temperature range, enable a reduction in the recommended
302 uncertainty for this reaction. We have combined the results of this study with that of Wennberg
303 et al. to report k_2(298 K) = (1.15 ± 0.19) × 10^{-11} cm^3 $molecule^{-1}$ s^{-1} and k_2(216–366 K) = 4.7 × 10^{-12} exp(274/T) cm^3 $molecule^{-1}$ s^{-1}, with f(298 K) = 1.08 and g = 40. Our recommended k_2(T) as
305 well as the 2σ uncertainty level is included in **Fig. 4**.

306 A few previous studies have investigated the branching ratio of reaction 2
307 [9,13,19,21,22]. Wennberg et al. measured the yield of O(^{3}P) atoms in an excess of N($^4S_{3/2}$)]
308 using O(^{3}P) resonance fluorescence detection. Their results suggest that the sole product channel
309 from reaction 2 is N_2O and O(^{3}P), channel 2a. Their approach, however, does not exclude the
310 possibility of channels 2b and 2c with nearly equal branching ratios. Clyne and McDermid
311 employed a discharge flow technique with mass spectrometric detection to monitor the formation
312 of N_2O, channel 2a. A kinetic simulation analysis yielded reasonable agreement with their
313 experimental results when the product channel ratio 2b/2a was <0.4. However, their final
314 recommendation for the channel 2b/2a ratio was 0, i.e., N_2O and O(^{3}P) being the only channel of
315 reaction 2. Kistiakowsky and Vopli [13] concluded that all three channels 2a-2c are active,
316 although not being quantitative. Phillips and Schiff [21] employed mass spectrometric detection
317 of reactant and products and is the only study to report channel 2d active with a yield of 0.13 ±
318 0.11. Our measurements show that the total O(^{3}P) yield, i.e., 2a branching ratio, is 0.66.
319 Combining our yield results with the observations of Wennberg et al., we conclude that the
320 branching ratio for reaction channels 2b and 2c to be ~0.17 each. The reported branching ratios
321 for reaction 2 have an estimated total uncertainty of ~9%.

322 This study has provided accurate experimental rate coefficient data for the N + NO and
323 NO_2 reactions over a range of temperature. The present results in combination with the previous
324 work of Wennberg et al. and Nakayama et al. provide the basis for the following recommended
325 rate coefficients; k_1(213–366 K) = 2.31 × 10^{-11} exp (134/T) cm^3 $molecule^{-1}$ s^{-1} and k_2(216–366 K)
326 = 4.7 × 10^{-12} exp (274/T) cm^3 $molecule^{-1}$ s^{-1}. In addition, the product branching ratio for the N +
327 NO_2 reaction was determined with the N_2O + O(^{3}P) channel found to account for 66% of the
328 product yield independent of temperature between 216 and 296 K.

Acknowledgements

This work was supported in part by NOAA Climate Program Office Atmospheric Chemistry, Carbon Cycle, and Climate Program and NASA's Atmospheric Composition Program.

Supplementary Material

* 2nd order plots for N + NO and N + NO_2 reactions at other temperatures in this study

Table 1

Summary of the experimental conditions and obtained rate coefficients for the $N(^4S_{3/2}) + NO(X^2\Pi)$ reaction

Temperature (K)	Pressure (Torr)	v (cm s^{-1})	$[N]_0$ [a]	$[O_2]$ [b]	[NO] [c]	k' range (s^{-1}) [d]	k(T) [e]
225	3.05	610	2.9	–	1.05–4.31 (5)	45–187	4.29 ± 0.24
225	2.09	618	2.6	4.4	0.82–4.03 (6)	34–168	4.19 ± 0.20
225	3.57	502	3.4	5.3	1.04 – 3.93 (5)	40–149	3.77 ± 0.30
							k (225 K) = 4.07 ± 0.13
237	3.06	614	2.7	–	0.96–3.94 (6)	36–141	3.82 ± 0.21
237	2.01	640	4.2	4.2	1.63–4.11 (5)	63–154	3.98 ± 0.34
							k (237 K) = 3.93 ± 0.17
251	3.11	676	4.3	–	1.63–4.75 (4)	70–184	3.48 ± 0.18
251	2.74	750	2.6	–	0.96–4.10 (6)	42–159	3.67 ± 0.15
251	2.53	740	4.0	–	1.48–4.46 (5)	66–163	3.93 ± 0.24
							k (251 K) = 3.62 ± 0.09
277	3.12	744	3.7	–	1.18–5.17 (5)	44–204	3.77 ± 0.10
277	2.54	818	3.5	–	1.60–3.90 (5)	53–133	3.36 ± 0.24
							k (277 K) = 3.56 ± 0.08
296	3.08	862	4.3	–	0.98–4.92 (5)	32–169	3.30 ± 0.09
296	5.56	445	3.1	–	0.75–3.41 (5)	27–121	3.65 ± 0.08
296	2.96	859	3.9	3.5	1.29–4.32 (5)	45–150	3.43 ± 0.12
296	4.09 [f]	1001	4.6	–	1.00–5.15 (5)	33–190	3.31 ± 0.07
							k (296 K) = 3.36 ± 0.04
344	3.21	766	4.6	–	1.58–3.89 (4)	63–161	3.92 ± 0.20
344	5.02	567	5.4	–	1.69–3.91 (5)	69–179	3.92 ± 0.24
344	2.71	1032	5.1	–	1.67–4.90 (5)	58–165	3.52 ± 0.13
344	2.16	980	2.9	–	1.05–4.15 (5)	45–155	3.72 ± 0.15
							k (344 K) = 3.63 ± 0.08

[a] units of 10^{11} molecule cm^{-3}, [b] units of 10^{14} molecule cm^{-3}, [c] units of 10^{12} molecule cm^{-3}, the number of $O(^3P)$ time profiles, i.e. number of NO concentrations, in each experiment is given in parenthesis, [d] corrected for axial diffusion loss, [e] units of 10^{-11} cm^3 $molecule^{-1}$ s^{-1}; the uncertainty is the 2σ precision of the linear least-squares fit to the data, [f] N_2 carrier gas was replaced with He

Table 2

Summary of the experimental conditions and obtained rate coefficients in this work for the $N(^4S_{3/2}) + NO_2(^2A_1)$ reaction

Temperature (K)	Pressure (Torr)	v (cm s^{-1})	$[N]_0$ [a]	$[O_2]$ [b]	$[NO_2]$ [c]	k' range (s^{-1}) [d]	k(T) [e]	$O(^3P)$ yield [f]
216	2.0	705	3.1	3.9	1.94–6.67 (6)	36–124	1.91 ± 0.07	0.64 ± 0.10
216	2.0	723	3.4	3.8	2.02–6.63 (6)	39–130	2.00 ± 0.08	0.67 ± 0.10
216	2.0	724	1.6	3.7	2.10–5.59 (5)	43–111	1.91 ± 0.12	0.64 ± 0.08
							k(216 K) = 1.95 ± 0.12	Yield(216 K) = 0.65 ± 0.10
237	2.0	784	2.5	3.5	2.19–8.87 (6)	31–131	1.45 ± 0.12	0.65 ± 0.04
							k(237 K) = 1.45 ± 0.12	Yield(237 K) = 0.65 ± 0.04
250	2.0	811	3.3	3.4	2.23–7.68 (6)	27–98	1.28 ± 0.06	0.67 ± 0.02
250	2.0	837	1.1	3.2	2.15–6.38 (6)	25–80	1.24 ± 0.08	0.67 ± 0.04
							k(250 K) = 1.27 ± 0.12	Yield(250 K) = 0.67 ± 0.03
296	2.0	961	3.0	2.9	2.36–8.91 (6)	25–101	1.17 ± 0.06	0.66 ± 0.04
296	2.0	976	3.3	2.9	2.50–8.80 (6)	33–108	1.21 ± 0.07	0.68 ± 0.06
296 [g]	2.0	985	3.8	3.2 [h]	2.26–7.55 (5)	29–94	1.23 ± 0.08	0.75 ± 0.06
296	4.1	707	3.2	4.0	3.89–7.40 (5)	39–75	1.01 ± 0.08	0.79 ± 0.06
296	4.1	700	2.9	6.0 [h]	2.46–8.58 (5)	25–87	1.02 ± 0.04	0.74 ± 0.04
							k(296 K) = 1.10 ± 0.06	Yield(296 K) = 0.72 ± 0.10

[a] units of 10^{11} molecules cm^{-3}, [b] units of 10^{14} molecules cm^{-3}, [c] units of 10^{12} molecules cm^{-3}, the number of $O(^3P)$ time profiles, i.e. number of NO_2 concentrations, in each experiment is given in parenthesis [d] corrected for axial diffusion loss, [e] units of 10^{-11} cm^3 $molecule^{-1}$ s^{-1} where the quoted uncertainty is the 2σ precision of the linear least-squares fit to the data, [f] quoted uncertainty is the 2σ measurement precision, 2σ, [g] Cl_2 added (~ 1.5 × 10^{14} molecules cm^{-3}), [h] O_2 replaced by SF_6

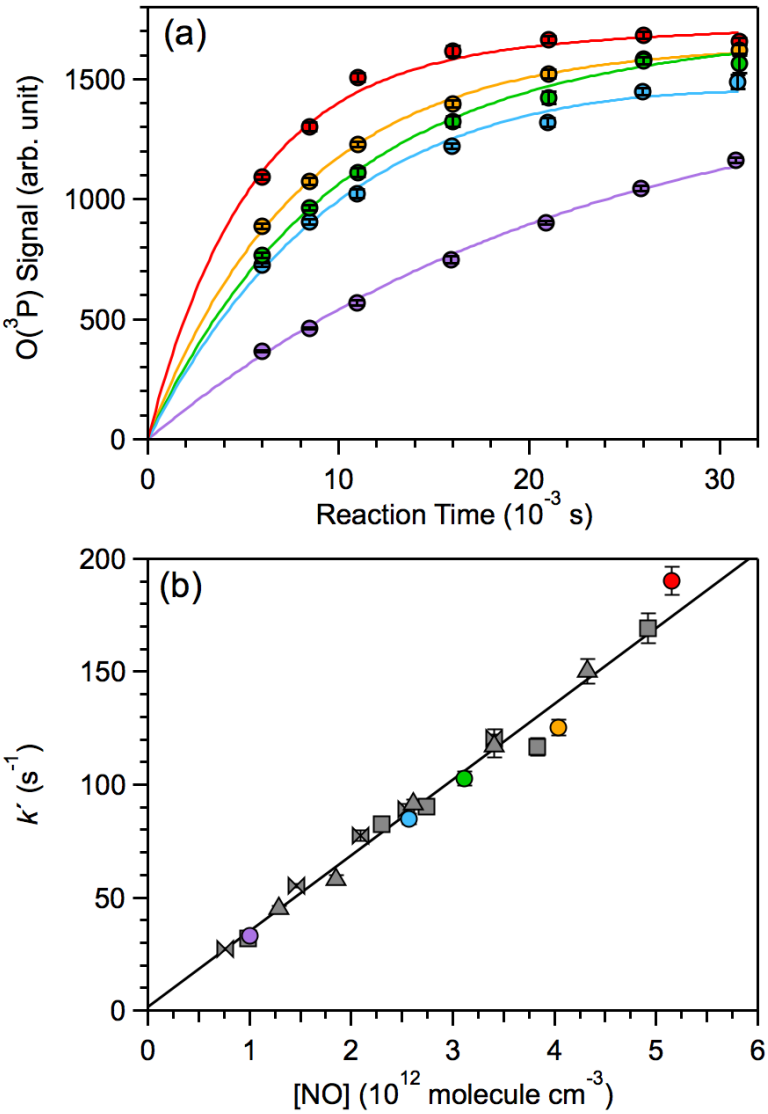

Fig. 1. Upper panel (a): Representative O(^{3}P) atom fluorescence signal profile for the N($^4S_{3/2}$) + NO($X^2\Pi$) reaction at 296 K. The different colors represent O(^{3}P) profiles at different NO concentration (in molecule cm^{-3}), [NO] = 9.99 × 10^{11} (purple), 2.57 × 10^{12} (light blue), 3.11 × 10^{12} (green), 4.03 × 10^{12} (brown) and 5.15 × 10^{12} (red) molecule cm^{-3}. The maximum O(^{3}P) atom fluorescence signal, S_{max}, for these profiles varied from 1606 to 1741 (arb. units). The errors shown represent the 2σ precision of the fluorescence signal measurement. Lower panel (b): Pseudo first-order rate coefficients, k'(296 K), for the N($^4S_{3/2}$) + NO($X^2\Pi$) reaction. The different symbols represent independent experiments performed over a range of experimental conditions, see **Table 1**. The colored symbols are the k'(296 K) from the fit of profiles shown in upper panel. The error bars represent the 2σ precision of the fits to the O(^{3}P) atom signal profiles.

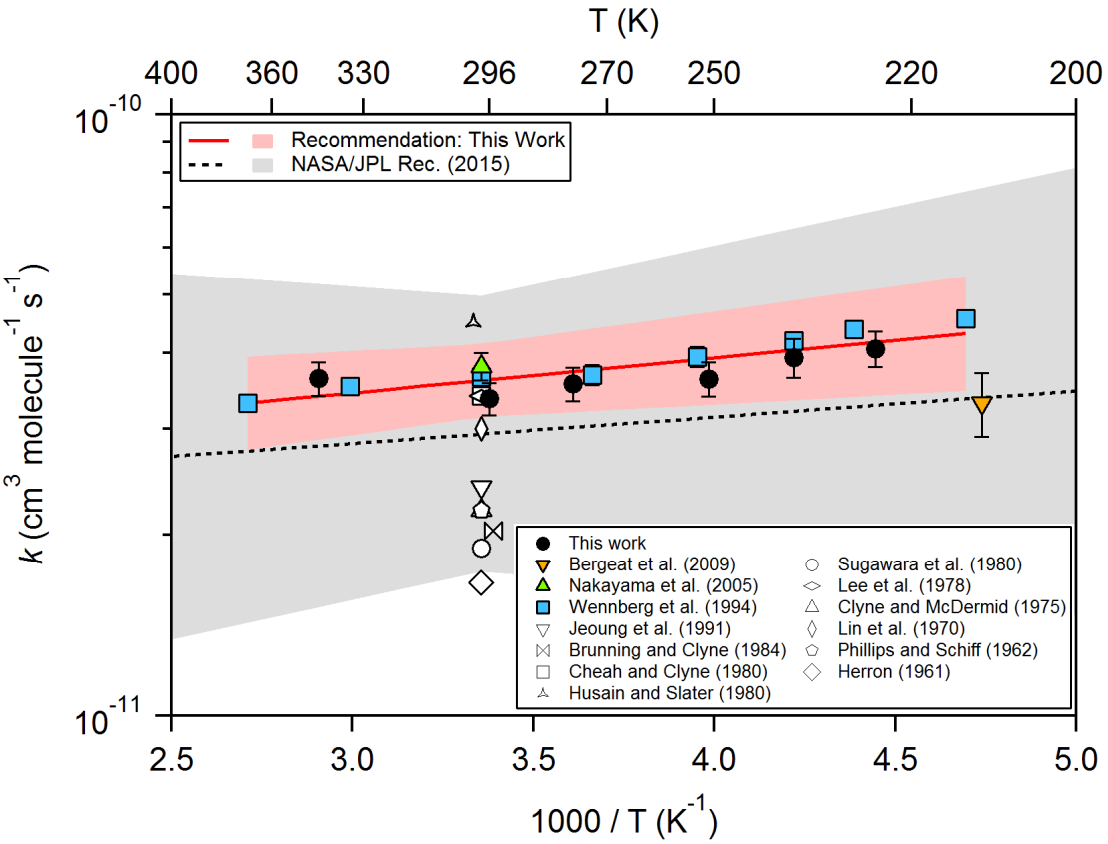

Fig. 2. Rate coefficient, *k*, data for the $N(^4S_{3/2}) + NO(X^2\Pi)$ reaction. The data from this work are shown along with 2σ total measurement uncertainty (solid black circles). The results and quoted uncertainties from the previous studies of Brunning and Clyne [7] (17), Cheah and Clyne [8] (18), Clyne and McDermid [9] (9), Herron [10] (48), Husain and Nigel [11] (4), Jeoung et al. [12] (8), Lee et al. [14] (26), Lin et al. [15] (33), Phillips and Schiff [17] (27), Sugawara et al. [18] (11), Wennberg et al. [19] (2), Nakayama et al. [16] (5), and Bergeat et al. [3] are included for comparison, where the values in parentheses are the reported percent uncertainties in their room temperature values (not included in graph for improved clarity). For the Lee et al. study, we have included the reported average rate coefficient and uncertainty. The NASA/JPL [6] recommendation (dashed black line and gray shaded area (2σ uncertainty)) is also included. The Arrhenius parameters and uncertainty levels recommended in this work are also shown (red solid line and red shaded area (2σ uncertainty)).

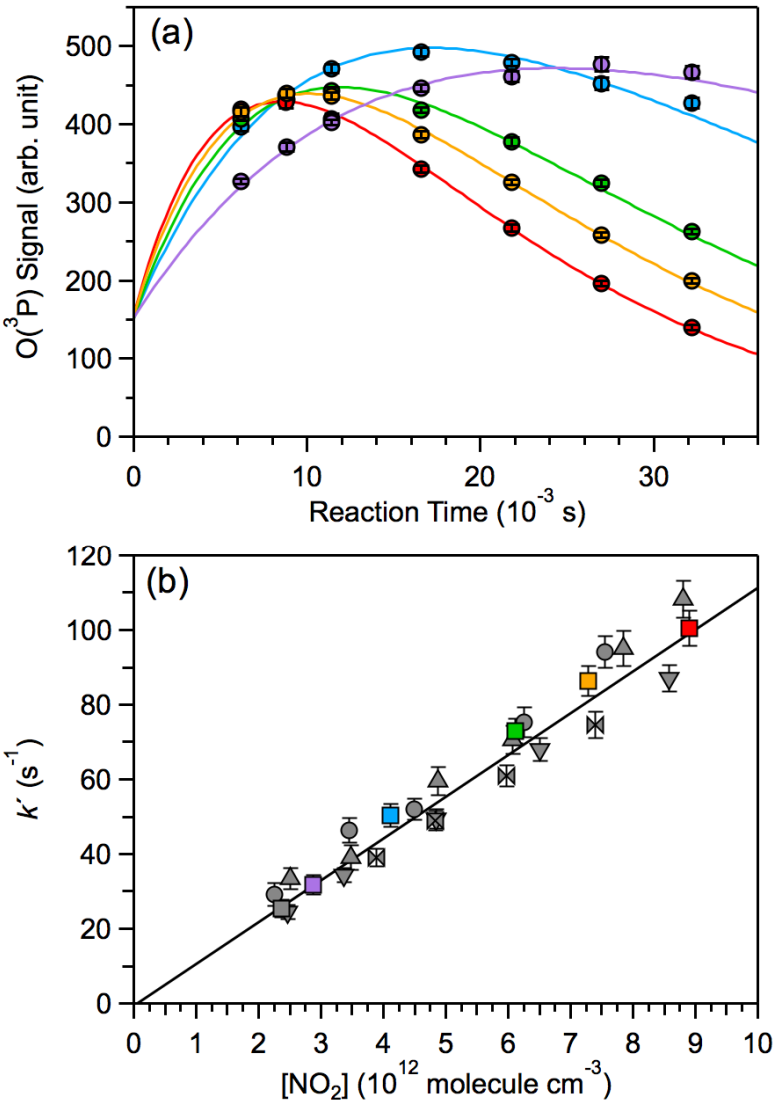

Fig. 3. Upper panel (a): Representative O(^{3}P) atom fluorescence signal profile for the N(^{4}S$_{3/2}$) + NO$_2$(^{2}A$_1$) reaction at 296 K. The different colors represent O(^{3}P) profiles at different NO$_2$ concentration (in molecules cm^{-3}), [NO$_2$] = 2.88 × 10^{12} (purple), 4.11 × 10^{12} (light blue), 6.12 × 10^{12} (green), 7.29 × 10^{12} (brown) and 8.91 × 10^{12} (red) molecules cm^{-3}. The maximum O(^{3}P) atom fluorescence signal, S_{max}, for these profiles was from 1244 to 1458 (arb. units). The errors shown represent the 2σ precision of the fluorescence signal measurement. Lower panel (b): Pseudo first-order rate coefficients, k'(296 K), for the N(^{4}S$_{3/2}$) + NO$_2$(^{2}A$_1$) reaction. The different symbols represent independent experiments performed over a range of experimental conditions, see **Table 2**. The colored symbols are the k'(296 K) from the fit of profiles shown in upper panel. The error bars represent the 2σ precision of the fits to the O(^{3}P) atom signal profiles.

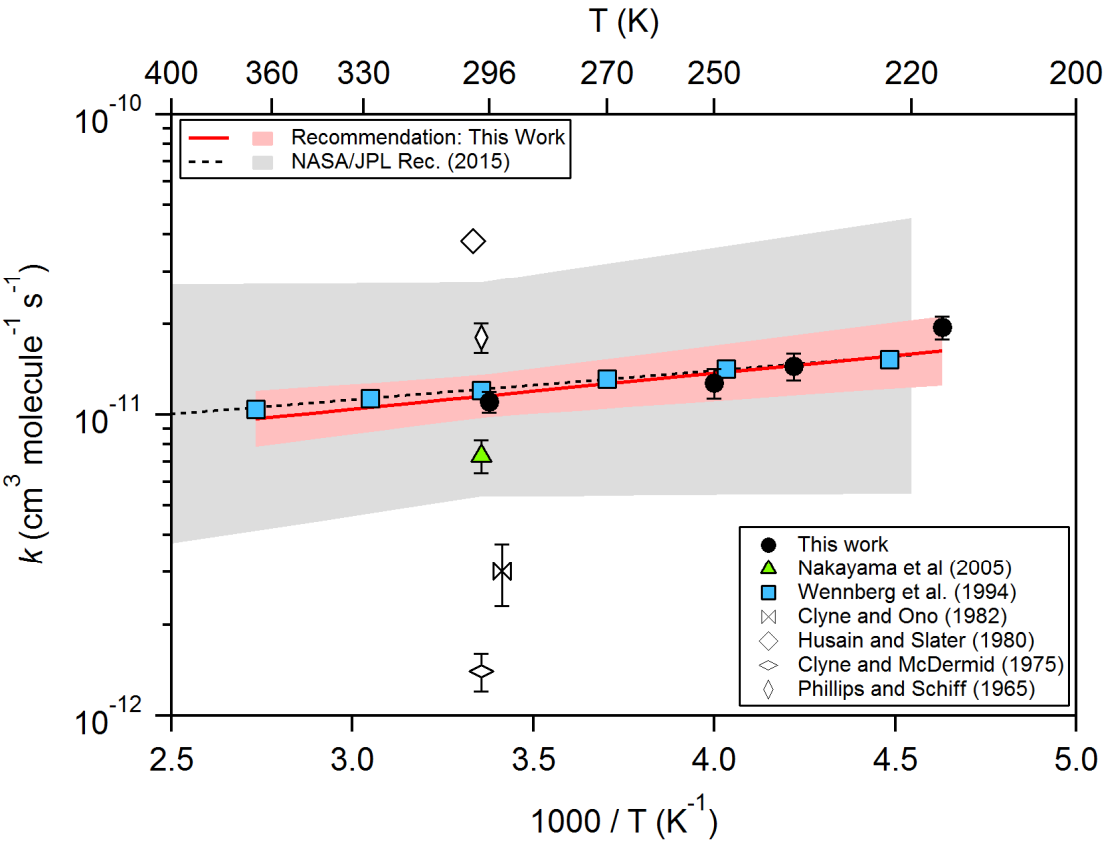

Fig. 4. Rate coefficients, *k*, for the $N(^4S_{3/2})$ + $NO_2(^2A_1)$ reaction. The data from this work are shown along with 2σ total measurement uncertainty (solid black circle). The results from the previous studies of Phillips and Schiff [17], Clyne and McDermid [9], Husain and Slater [11], Clyne and Ono [20], Wennberg et al. [19], and Nakayama et al. [16] are included for comparison. The NASA/JPL [6] recommendation (dashed black line and shaded area (2σ uncertainty)) is also included. The Arrhenius parameters and uncertainty levels recommended in this work are also shown (red solid line and shaded area, 2σ uncertainty).

References

[1] P.J. Crutzen, The role of NO and NO_2 in the chemistry of the troposphere and stratosphere, Ann. Rev. Earth and Planetary Sciences (1979)

[2] D.E. Siskind, D.W. Rusch, Nitric oxide in the middle to upper thermosphere, J. Geophys. Res. 97 (1992) 3209-3217.

[3] A. Bergeat, K.M. Hickson, N. Daugey, P. Caubet, M. Costes, A low temperature investigation of the N(^{4}S°) + NO reaction, Phys. Chem. Chem. Phys. 11 (2009) 8149-8155.

[4] J.L. Fox, Rate coefficient for the reaction N + NO, J. Geophys. Res. 99 (1994) 6273-6276.

[5] J.-C. Gérard, Thermospheric odd nitrogen, Planetary Space Sciences 40 (1992) 337-353.

[6] J.B. Burkholder, S.P. Sander, J. Abbatt, J.R. Barker, R.E. Huie, C.E. Kolb, M.J. Kurylo, V.L. Orkin, D.M. Wilmouth, P.H. Wine, Chemical Kinetics and Photochemical Data for Use in Atmospheric Studies, Evaluation No. 18, JPL Publication 15-10 (2015).

[7] J. Brunning, M.A. Clyne, Elementary reactions of the SF radical. Part 1.—Rate constants for the reactions F + OCS → SF+ CO and SF+ SF→ SF_2 + S, J. Chem. Soc., Faraday Trans. 2 80 (1984) 1001-1014.

[8] C.T. Cheah, M.A. Clyne, Reactions forming electronically-excited free radicals. Part 2.—Formation of N $_4$S, N ^{2}D and N ^{2}P atoms in the H + NF_2 reaction, and N atom reactions, J. Chem. Soc., Faraday Trans. 2 76 (1980) 1543-1560.

[9] M.A. Clyne, I.S. McDermid, Mass spectrometric determinations of the rates of elementary reactions of NO and of NO_2 with ground state N ^{4}S atoms, J. Chem. Soc., Faraday Trans. 1 71 (1975) 2189-2202.

[10] J.T. Herron, Rate of the Reaction NO + N, J. Chem. Phys. 35 (1961) 1138-1139.

[11] D. Husain, N.K.H. Slater, Kinetic study of ground state atomic nitrogen, N($^4S_{3/2}$), by time-resolved atomic resonance fluorescence, J. Chem. Soc., Faraday Trans. II 76 (1980) 606-619.

[12] S.C. Jeoung, K.Y. Choo, S.W. Benson, Very-low-pressure-reactor chemiluminescence studies on nitrogen atom reactions with chloroform and deuteriochloroform, J. Phys. Chem. 95 (1991) 7282-7290.

[13] G.B. Kistiakowsky, G.G. Volpi, Reactions of nitrogen atoms. II. H_2, CO, NH_3, NO, and NO_2, J. Chem. Phys. 28 (1958) 665-668.

[14] J.H. Lee, J.V. Michael, W.A. Payne, L.J. Stief, Absolute rate of the reaction of N(^4S) with NO from 196–400 K with DF–RF and FP–RF techniques, J. Chem. Phys. 69 (1978) 3069-3076.

[15] C.L. Lin, D.A. Parkes, F. Kaufman, Oscillator strength of the resonance transitions of ground-state N and O, J. Chem. Phys. 53 (1970) 3896-3900.

[16] T. Nakayama, K. Takahashi, Y. Matsumi, K. Shibuya, N(^{4}S) formation following the 193.3-nm ArF laser irradiation of NO and NO_2 and its application to kinetic studies of N(^{4}S) reactions with NO and NO_2, J. Phys. Chem. A 109 (2005) 10897-10902.

[17] L.F. Phillips, H.I. Schiff, Mass spectrometric studies of atom reactions. I. Reactions in the atomic nitrogen-ozone system, J. Chem. Phys. 36 (1962) 1509-1517.

[18] K. Sugawara, Y. Ishikawa, S. Sato, The rate constants of the reactions of the metastable nitrogen atoms, ^{2}D and ^{2}P, and the reactions of N(^{4}S) + NO → N_2 + O(^{3}P) and O(^{3}P) + NO + M → NO_2 + M, Bull. Chem. Soc. Japan 53 (1980) 3159-3164.

[19] P.O. Wennberg, J.G. Anderson, D.K. Weisenstein, Kinetics of Reactions of Ground State Nitrogen Atoms ($^4S_{3/2}$) with NO and NO_2, J. Geophys. Res. 99 (1994) 18839-18846.

[20] M.A. Clyne, Y. Ono, Determination of the rate constant of reaction of $N(^4S_{3/2})$ with NO_2 using resonance fluorescence in a discharge flow system, Chem. Phys. 69 (1982) 381-388.
[21] L.F. Phillips, H.I. Schiff, Mass-spectrometric studies of atomic reactions. V. The reaction of nitrogen atoms with NO_2, J. Chem. Phys. 42 (1965) 3171-3174.
[22] M.-H. Zuo, H.-L. Liu, X.-R. Huang, J.-L. Li, C.-C. Sun, Atomic radical–molecule reaction N (^4S) + NO_2 ($^2A_1$): Mechanistic study, Chem. Phys. 358 (2009) 80-84.
[23] C.J. Howard, Kinetic measurements using flow tubes, J. Phys. Chem. 83 (1979) 3-9.
[24] D.K. Papanastasiou, J.B. Burkholder, Rate Coefficients for the $O(^3P)$ + Cl_2O Gas-Phase Reaction between 230 and 357 K, Int. J. Chem. Kinet. 43 (2011) 312-321.
[25] D.K. Papanastasiou, K.J. Feierabend, J.B. Burkholder, Cl_2O photochemistry: Ultraviolet/vis absorption spectrum temperature dependence and $O(^3P)$ quantum yield at 193 and 248 nm, J. Chem. Phys. 134 (2011) 204310.
[26] I.C. Plumb, K.R. Ryan, N.G. Barton, Method for the measurement of diffusion coefficients of labile gas-phase species: The diffusion coefficient of $O(^3P)$ in He at 294 K, Int. J. Chem. Kinet. 15 (1983) 1081-1097.
[27] T.G. Slanger, B.J. Wood, G. Black, Temperature coefficients for $N(^2D)$ quenching by O_2 and N_2O, J. Geophys. Res. 76 (1971) 8430-8433.
[28] R. Iwata, R.A. Ferrieri, A.P. Wolf, Rate constant determination of the reaction of metastable $N(^2D,^2P)$ with NO_2 using moderated nuclear recoil atoms, J. Phys. Chem. 90 (1986) 6722-6726.
[29] D.L. Baulch, C.T. Bowman, C.J. Cobos, R.A. Cox, T. Just, J.A. Kerr, M.J. Pilling, J. Troe, W. Tsang, R.W. Walker, J. Warnatz, Evaluated kinetic data for combustion modeling. Supplement II, J. Phys. Chem. Ref. Data 34 (2005) 757-1397.

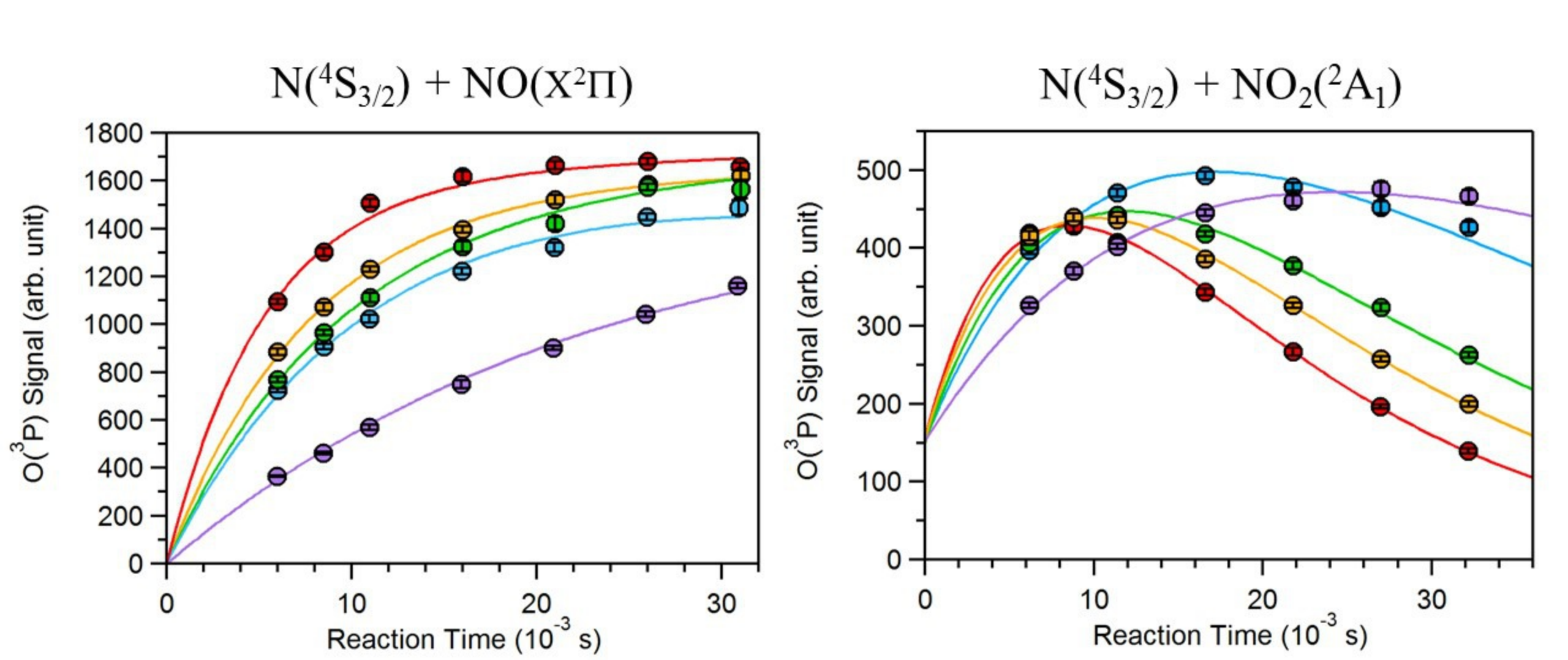
N(4S3/2) + NO(X2Π)
O(3P) Signal (arb. unit)
Reaction Time (10-3 s)
0
200
400
600
800
1000
1200
1400
1600
1800
0
10
20
30
N(4S3/2) + NO2(2A1)
O(3P) Signal (arb. unit)
Reaction Time (10-3 s)
0
100
200
300
400
500
0
10
20
30